

Development of Thermal Control Systems for The Space-borne Optical Payload for New Possibilities and Opportunities for Nanosatellites Applications

Jin-Soo Chang

*Thermal Control Systems
of Dept. of Satellite Systems
TelePIX Co., Ltd.*

Daejeon, Republic of Korea
garry.jin.s.chang@telepix.net

(ORCID: 0009-0008-5013-1363)

Dong-Jun Choi

*Opto-Mechanical Systems
of Dept. of Satellite Systems
TelePIX Co., Ltd.*

Daejeon, Republic of Korea
choidj@telepix.net

Minwook Joo

*Opto-Mechanical Systems
of Dept. of Satellite Systems
TelePIX Co., Ltd.*

Daejeon, Republic of Korea
jmw@telepix.net

Sehyun Seong

Dept. of Satellite Systems

TelePIX Co., Ltd.
Daejeon, Republic of Korea
shseong@telepix.net

Ohgan Kim

*Opto-Mechanical Systems
of Dept. of Satellite Systems
TelePIX Co., Ltd.*

Daejeon, Republic of Korea
ohgankim@telepix.net

Seonghui Kim

Dept. of Satellite Systems

TelePIX Co., Ltd.
Daejeon, Republic of Korea
barlow@telepix.net

Abstract: Based on the many years of accumulated development experiences of space program, TelePIX has successfully developed *Space-borne Optical Payload (SOP)* for a 6U-class Nanosatellite platform. SOP consists of the *Data Processing and Handling Unit (DPHU)* which is used for the interface of telecommunication with the platform, and the *Optical Head (OH)* which is used for the image taking and processing.

SOP was designed to provide the image of PAN/MS 5.0 m resolution respectively with more than 50 SNR performance at a design altitude of 500 km despite of 3U sized and less than 4 kg. The thermal control systems for SOP was realized through a passive thermal control design, which was optimized based on various case studies to minimize power consumption of SOP. In addition, a derating review about major EEE parts used in SOP was conducted based on the part level thermal analysis of the electronics. Thermo-elastic analysis of the OH was also carried out by mapping the results of the thermal analysis onto the structural analysis model.

To evaluate thermal performance and integrity, and workmanship of the *Flight Model (FM)* under the acceptance level, we performed the thermal vacuum test combined by thermal vacuum cycling tests and thermal balance tests. The thermal vacuum cycling tests were completed without any issues. The evaluation of thermal analysis model for the SOP was performed by comparing the results with thermal balance test results in accordance with ECSS standard. After the correlation process, the deviations between the test and analysis results were satisfied the criteria.

Currently, we are waiting for the launch and LEOP activities scheduled in January/February 2025.

Keywords: *Bluebon, Space-borne Optical Payload, SOP, Electro-Optical Camera, Thermal Control Systems, TCS, Thermal Vacuum Cycling Test, Thermal Balance Test, TMM Tuning, TelePIX*

I. INTRODUCTION

TelePIX has developed a compact electro-optical camera system called the *Space-borne Optical Payload (SOP)*, which

is applicable to Nano- and Microsatellites. The SOP comprises the *Optical Head (OH)*, which is an electro-optics, and the *Data Processing and Handling Unit (DPHU)*, which is an electronics. Despite its small size of approximately $100 \times 100 \times 300 \text{ mm}^3$ (i.e., roughly equivalent to 3U), the SOP is a high-performance electro-optical camera system capable of capturing the image with a resolution of 5.0 meters for both *Panchromatic (PAN)* and *Multi-spectral (MS)* bands from an altitude of 500 km.

The *Flight Model (FM)* of SOP was developed with the goal of being launched on Space-X's Transporter-12 mission, and the thermal vacuum test was conducted with acceptance level. The thermal vacuum test consisted of 4 cycles of thermal vacuum cycling tests and 2 thermal balance tests. Through the thermal vacuum cycling tests, thermal performance and integrity of the SOP were verified. In addition, based on the results of the thermal balance tests, the thermal analysis model was evaluated and validated, confirming that it accurately represents the thermal characteristics of the SOP.

This paper presents the development process and results of the thermal control systems for the SOP, which has the potential to provide new possibilities and opportunities for performing Earth observation missions utilizing nanosatellites.

II. DEVELOPMENT OF THERMAL CONTROL SYSTEMS

To carry out "*Bluebon*" mission, which observes "*Blue Carbon*", a carbon sink in marine ecosystems, the SOP is integrated into a 3U-sized platform as shown in Fig. 1 and operated in the mission orbit. Based on the agreed interface temperature with the platform and the space thermal environment of the mission orbit, design and analysis for the thermal control systems were conducted separately for the OH and DPHU. The detailed outline is as follows.

A. Optical Head (OH)

For the OH, which is an electro-optics, the bus interface temperature was defined as $-5 \sim 35 \text{ }^\circ\text{C}$ based on the agreement with the platform, and the satellite operates in "*HK Mode*"

under nominal conditions and switches to “*IMG Mode*” for image capturing as shown in Fig. 2 [1-2].

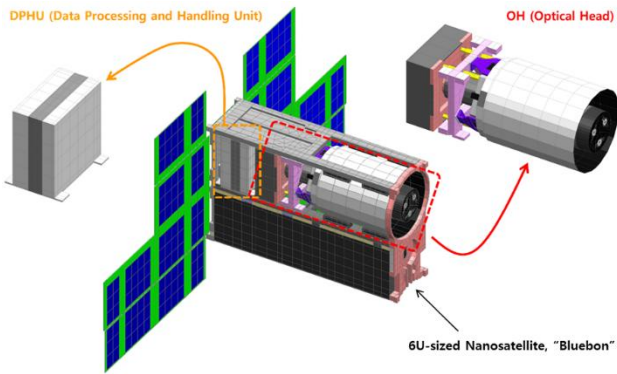


Fig. 1. 6U-sized Nanosatellite for Bluebon Mission

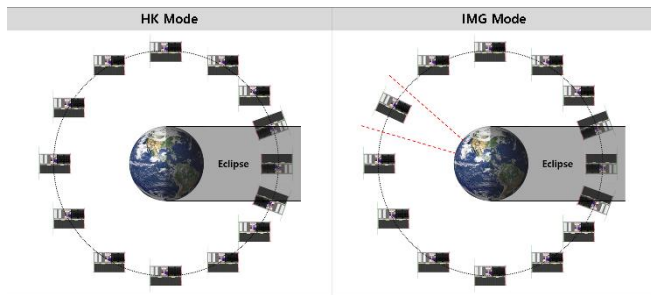


Fig. 2. On-Orbit Satellite Attitude depending on Operation Mode

However, from the perspective of the development of thermal control systems, although the satellite attitude changes from “*Max. Sun Tracking*” to “*Earth Pointing*” for image capturing, the change in the orbital thermal environment due to the satellite attitude change is not significant because it is during the daylight. Furthermore, the duration of satellite’s attitude change including the imaging period, is less than two minutes, which is relatively short by comparing with an orbital period. Therefore, orbital thermal analysis for both “*HK Mode*” and “*IMG Mode*” was conducted based on “*HK Mode*” to simplify the thermal analysis model.

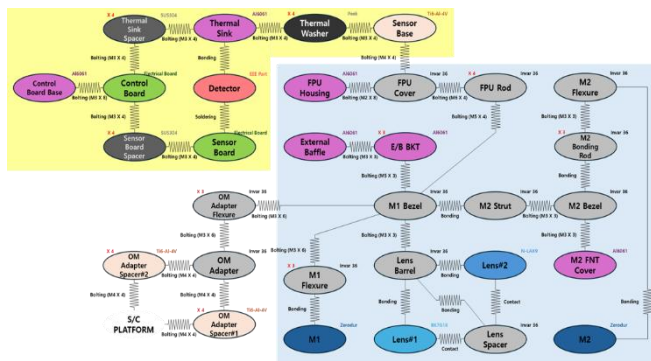


Fig. 3. Thermal Network Analysis Result: OH

To model the thermal analysis model, thermal couplings between individual parts of OH were reviewed based on the opto-mechanical design and assembly method of the OH, and the thermal network was derived as shown in Fig. 3 [1]. Based on this, thermal coupling conditions between individual parts were analyzed and the results of major parts are summarized in TABLE I.

TABLE I. THERMAL COUPLING ANALYSIS RESULT

Thermal Coupling	Value (K/W)
M1 Bezel-2-M1 Flexure	0.64
M1 Flexure-2-M1	1.34
M1 Bezel-2-Lens_Barrel	1.28
Lens_Barrel-2-Lens#1	1.01
Lens_Barrel-2-Lens#2	0.65
M1 Bezel-2-M2 Strut	0.34
M2 Strut-2-M2 Bezel	1.28
M2 Bezel-2-M2_Bonding_Rod	1.49
M2_Bonding_Rod-2- M2 Flexure	1.28
M2 Flexure-2-M2	9.77
M1 Bezel-2-External Baffle BKT	0.25
E/B BKT-2-External_Baffle	1.28

During the image capturing, the SOP was exposed to dissipated heat depending on operating profile as shown in Fig. 4, and this heat dissipation condition was defined based on the satellite’s pass time over the primary target area, the Korean Peninsula, located at 30 degrees north latitude for “*IMG Mode*”.

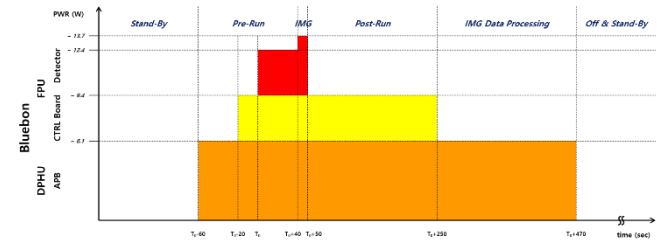


Fig. 4. Heat Dissipation depending on Operating Profile of IMG Mode

Based on the above processes, **thermal analysis model (TAM)** was modeled from 3D CAD model using “*SIEMENS NX (ver. 2306)*”, as shown in Fig. 5, and the thermal boundary conditions were defined using “*SPACE SYSTEMS THERMAL (ver. 2306, Build 177143)*” pre/post application [3-4].

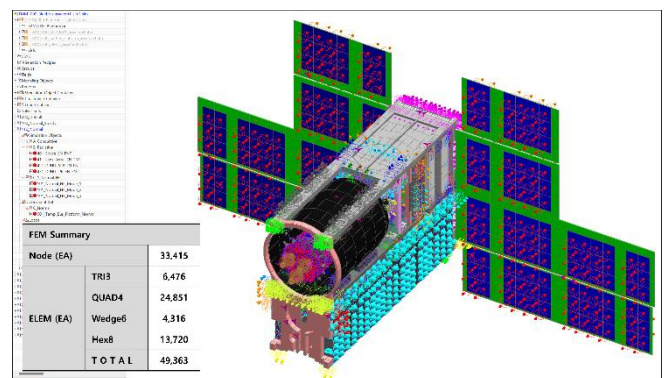


Fig. 5. Thermal Analysis Model of the SOP with the Platform

Based on the analysis results, the maximum temperature deviation between **primary mirror (M1)** and **secondary mirror (M2)** which are critical components affecting image quality, was reviewed about daylight period when imaging takes place.

As shown in Fig. 6, the spatial difference was approximately 5.5 degrees K. In addition, the temporal difference of major optical components during imaging operation was checked, revealing approximately 2.2 degrees K at the detector as shown in Fig. 7. Both the spatial and temporal differences are within the acceptable limits defined by the OH's opto-mechanical requirements, confirming that the current design is sufficient [2].

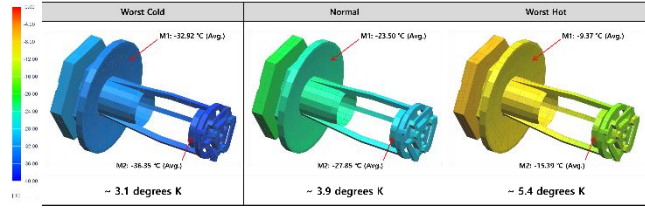


Fig. 6. Spatial Difference on Metering Structure and Mirrors

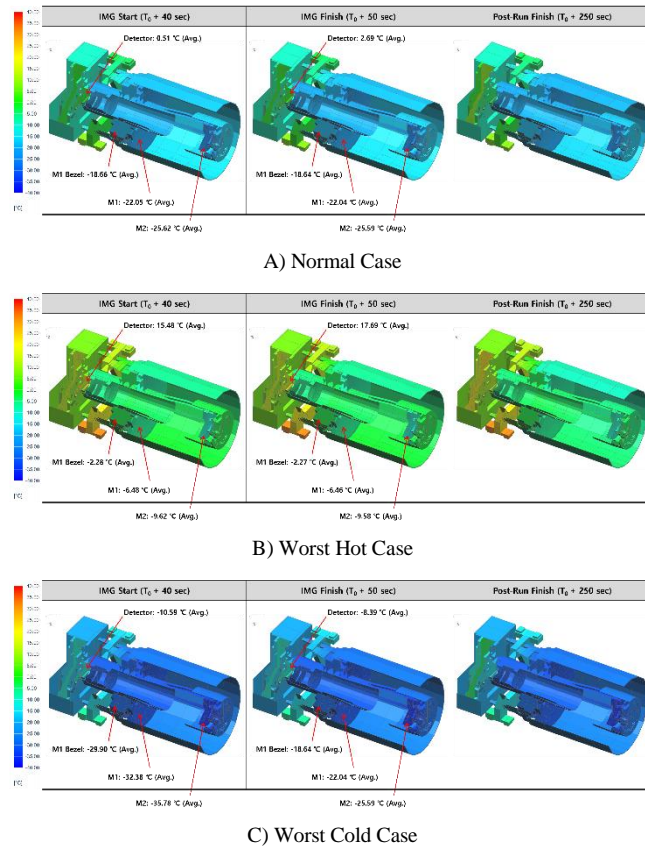


Fig. 7. Temporal Difference on OH before/after Imaging Operation

In case of the expected on-orbit temperatures, they are depicted in Fig. 8 for each analysis case respectively and the anticipated temperature ranges during the whole mission period are summarized in TABLE II.

As shown in TABLE II, the minimum temperature of the detector is -18.6°C , which satisfies the requirement of being above -20°C [5]. However, considering uncertainties arising from the thermal analysis model and thermally conductive and radiative interactions with the platform, a temperature margin of at least 5 degrees K was deemed necessary. Therefore, to ensure that the detector temperature remains above -15°C , the *vacuum deposited-aluminum (VDA)* coating was applied to the external surface of "External Baffle". As a result, the minimum expected temperature of the detector was adjusted to approximately -13°C , as shown in TABLE III.

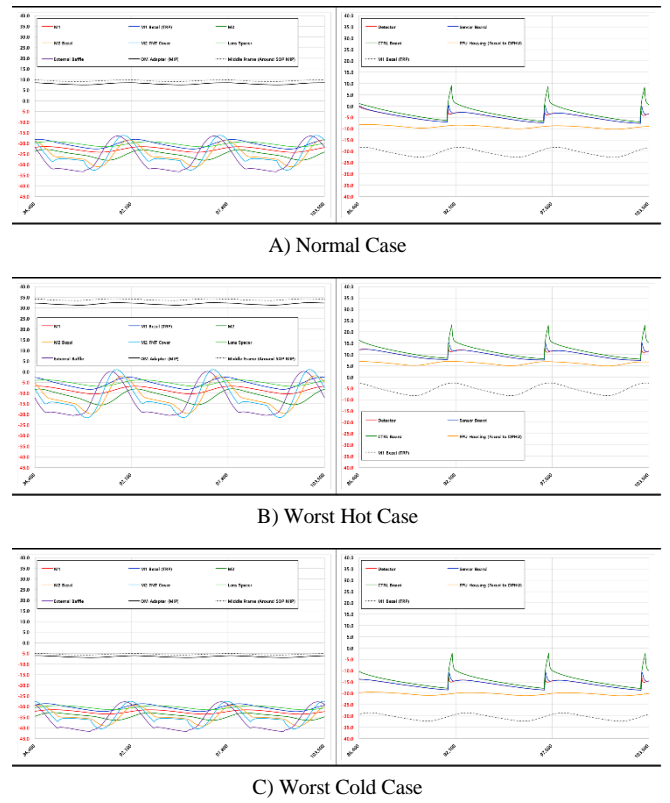


Fig. 8. On-Orbit Expected Temperature Profile of OH

TABLE II. ON-ORBIT EXPECTED TEMPERATURE RESULT

Major Part	Expected Temperature ($^{\circ}\text{C}$)
M1	-33.53 ~ -6.74
M1 Bezel	-32.32 ~ -2.52
M2	-36.41 ~ -7.98
M2 Bezel	-39.08 ~ -1.86
External Baffle	-41.70 ~ 0.19
Detector	-18.58 ~ 13.25
Sensor Board	-18.56 ~ 15.41
Control Board	-17.83 ~ 23.16

TABLE III. ON-ORBIT EXPECTED TEMPERATURE RESULT (REVISED)

Major Part	Expected Temperature ($^{\circ}\text{C}$)
M1	-33.53 ~ -6.74
M1 Bezel	-32.32 ~ -2.52
M2	-36.41 ~ -7.98
M2 Bezel	-39.08 ~ -1.86
External Baffle	-41.70 ~ 0.19
Detector	-18.58 ~ 13.25
Sensor Board	-18.56 ~ 15.41
Control Board	-17.83 ~ 23.16

B. Data Processing and Handling Unit (DPHU)

For the DPHU, which is an electronics, it is common to conduct a conservative review based on steady-state analysis

to account for uncertainties in estimation of dissipated power of EEE parts and operational time. However, in case of SOP, since the operating duration for the image capturing is relatively short, such an approach may lead to over-design. Therefore, transient analysis was performed based on the operating profile and the results are summarized in Fig. 9 and TABLE IV.

As seen in the results, the maximum temperatures of each major EEE parts were observed at the end of *"IMG Data Processing"* phase and sufficient temperature margins were confirmed for both operating and junction temperatures.

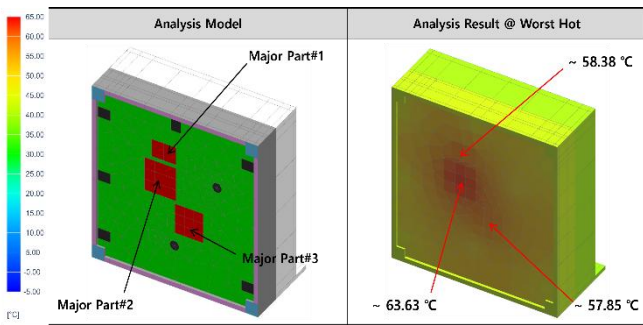


Fig. 9. Temperature Distribution at the End of IMG Data Processing

TABLE IV. EEE PART THERMAL COMPLIANCE CHECK: OPERATING

EEE Part	Specification			Expectation		Compliance
	T_O^a	T_J^b	θ_{JB}^c	T_O	T_J	
Major Part#1	~ 85	~ 125	3.8	~ 58.4	~ 62.2	Complied
Major Part#2	~ 100	~ 135	3.2	~ 63.6	~ 73.2	Complied
Major Part#3	~ 100	~ 100	3.0	~ 57.9	~ 59.4	Complied

- a. Max. Operating Temperature (°C)
- b. Max. Junction Temperature, Absolute (°C)
- c. Junction-2-Board Thermal Resistance (K/W)

Next, derating review about major EEE parts was performed based on [6]. For this review, the platform temperature, which serves as the baseplate for DPHU, was set to 45°C based on the acceptance hot test temperature and the results are summarized in TABLE V.

TABLE V. EEE PART THERMAL COMPLIANCE CHECK: DERATING

EEE Part	Specification			Expectation		Compliance
	T_O	T_{JD}^d	θ_{JB}	T_O	T_J	
Major Part#1	~ 85	~ 85	3.8	~ 68.4	~ 72.2	Complied
Major Part#2	~ 100	~ 95	3.2	~ 73.6	~ 83.2	Complied
Major Part#3	~ 100	~ 60	3.0	~ 67.9	~ 69.4	Non-Complied

- d. Max. Junction Temperature, Derated (°C)

According to TABLE V, unlike *"Major Part#1"* and *"#2"*, *"Major Part#3"* was found to have an issue with temperature margin in terms of junction temperature.

However, considering the mission duration is relatively short as 1 year, and that there is a sufficient temperature margins of over 30 degrees K under operating conditions, it was determined that requiring full compliance including derating conditions for this mission would be excessive.

Therefore, the design was accepted without modification through a waiver.

III. VALIDATION AND EVALUATION OF THERMAL CONTROL SYSTEMS

After FM was finalized, we conducted the thermal vacuum test, consisting of 4 cycles of thermal vacuum cycling test and 2 thermal balance tests to evaluate thermal performance and integrity, and the workmanship under the acceptance test level, as shown in Fig. 10.

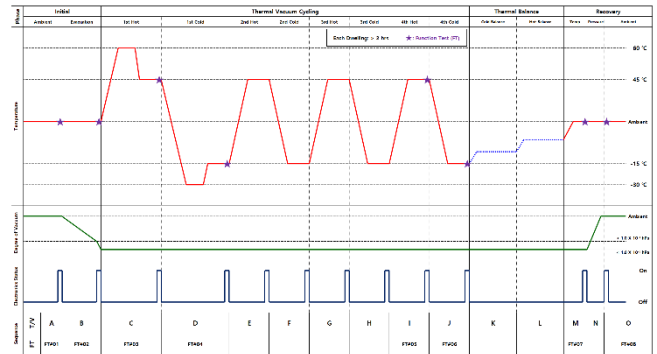


Fig. 10. Thermal Vacuum Test Profile for SOP FM

The thermal vacuum test was planned to be conducted for both the Flight Model for launch (FM#1) and the redundancy (FM2) simultaneously. To ensure successful test conducting, the analysis model for thermal vacuum test was modeled, as shown in Fig. 11, and a preceding review was carried out [7].

Based on review results, the test configuration, including test jig and test heaters, and the test conducting plan were established. Fig. 12 shows the test configuration, and Fig. 13 presents the results of the preceding review.

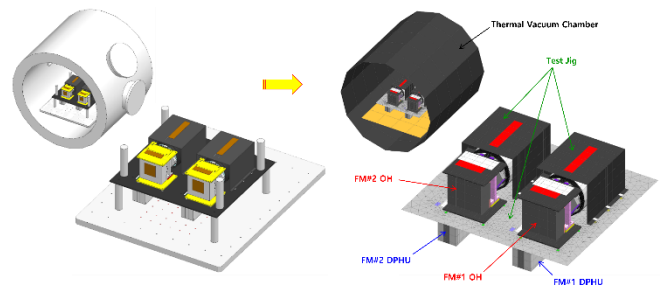


Fig. 11. Analysis Model for Thermal Vacuum Test

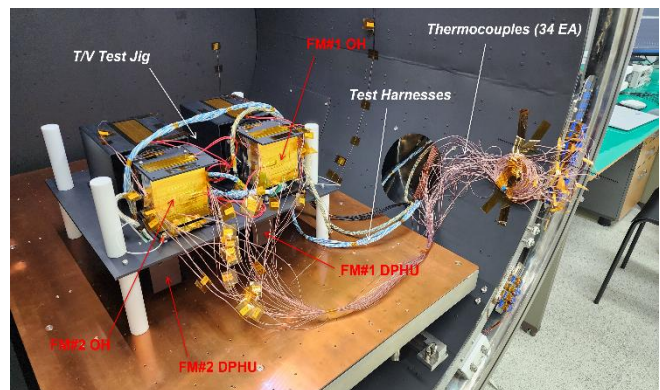


Fig. 12. Test Setup Configuration of SOP FM Thermal Vacuum Test

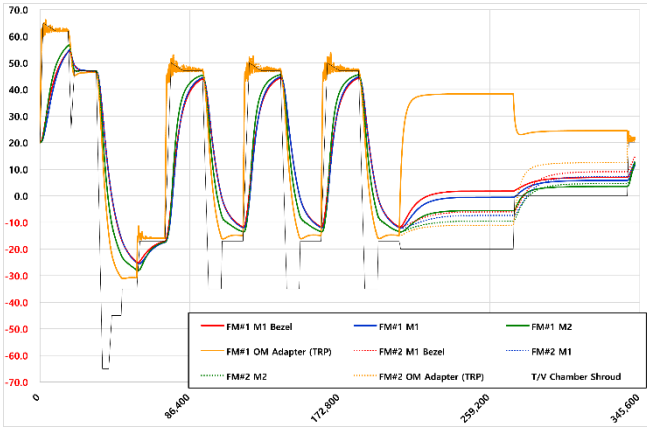


Fig. 13. Result of Preceding Thermal Analysis for Thermal Vacuum Test

The thermal balance test is conducted twice, as cold balance and hot balance. From the perspective of validating the thermal analysis model, thermal balance tests were conducted by applying different test conditions to FM#1 and FM#2, allowing us to achieve the equivalent effect of obtaining 4 thermal balance test results.

The thermal vacuum test was completed within test requirements as shown in Fig. 14. By comparing the *Modulation Transfer Function (MTF)* measurement results taken before and after the thermal vacuum test, it was confirmed that there were no anomalies on the SOP.

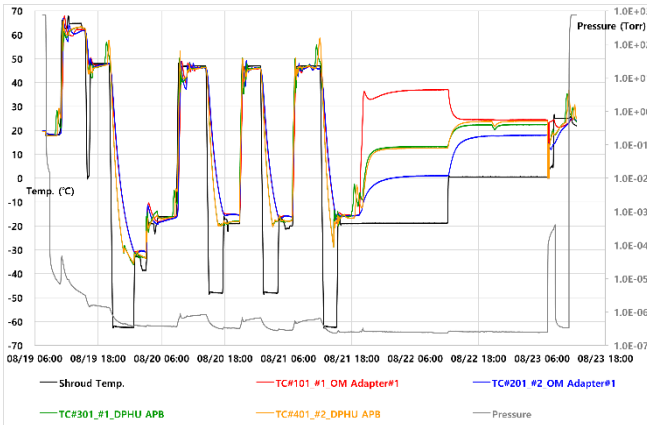


Fig. 14. SOP FM Thermal Vacuum Test Result

Next, the validation of the thermal analysis model for the OH based on the thermal balance test results is discussed. To evaluate the thermal analysis model, a correlation was performed by updating the analysis model for thermal vacuum test to reflect the actual test configuration and boundary conditions. After analysis model tuning, we compared the analysis results from correlated model with the thermal balance test results as summarized in TABLE VI. Also, the evaluation based on ECSS confirmed that all of evaluation requirements were satisfied as shown in TABLE VII [8].

IV. CONCLUSION

TelePIX has successfully completed the design and development of a 3U-class compact electro-optical camera system, SOP, which can be applied to Nano- and Micro-satellites. For the thermal control systems, its design was tailored to the specific characteristics of both OH and DPHU

comprising the SOP and its performance was verified through thermal vacuum test and comparison of MTF measurement results taken before and after the test. Additionally, thermal balance test results were used to evaluate and validate the thermal analysis model.

TABLE VI. ANALYSIS VS. THERMAL BALANCE TEST RESULT

ID	Description	Cold Balance			Hot Balance		
		T/R ^e	A/R ^f	De. ^g	T/R	A/R	De.
#101	#1_OM Adapter#1	33.26	37.99	-4.73	22.59	24.88	-2.29
#102	#1_OM Adapter#2	37.00	40.24	-3.24	24.45	25.59	-1.14
#103	#1_OM A Flexure	31.80	27.41	4.39	20.90	19.47	1.43
#104	#1_M1 Bezel	19.20	19.45	-0.25	14.86	15.62	-0.76
#105	#1_Lens Barrel, U	20.20	19.27	0.93	15.27	15.58	-0.31
#106	#1_Lens Barrel, L	19.00	19.19	-0.19	14.92	15.57	-0.65
#107	#1_FPU Cover	11.71	14.71	-3.00	12.84	15.00	-2.16
#1-A	#1_FPU_CEM	17.23	20.58	-3.35	-	20.90	-
#1-B	#1_FPU_FEE	15.13	18.24	-3.11	-	18.50	-
#108	#1_FPU Housing	10.40	13.87	-3.47	12.30	14.59	-2.29
#109	#1_M2 Cover	11.34	10.03	1.31	9.85	10.55	-0.70
#110	#1_E/B BKT	16.80	17.29	-0.49	13.26	14.30	-1.04
#111	#1_External Baffle	17.00	14.75	2.25	12.52	12.72	-0.20
#201	#2_OM Adapter#1	1.00	-0.15	1.15	17.94	17.55	0.39
#202	#2_OM Adapter#2	1.70	-1.69	3.39	15.89	16.59	-0.70
#203	#2_OM A Flexure	-2.70	1.11	-3.81	15.32	15.79	-0.47
#204	#2_M1 Bezel	4.09	3.00	1.09	14.79	15.25	-0.46
#205	#2_Lens Barrel, U	4.17	2.99	1.18	15.58	15.26	0.32
#206	#2_Lens Barrel, L	4.36	2.97	1.39	15.12	15.28	-0.16
#207	#2_FPU Cover	14.60	12.12	2.48	26.20	24.94	1.26
#2-A	#2_FPU_CEM	19.73	18.29	1.44	-	30.77	-
#2-B	#2_FPU_FEE	16.00	15.65	0.35	-	28.27	-
#208	#2_FPU Housing	15.80	13.04	2.76	27.95	25.97	1.98
#209	#2_M2 Cover	1.63	0.84	0.79	10.59	10.84	-0.25
#210	#2_E/B BKT	3.91	3.01	0.90	13.86	14.16	-0.30
#211	#2_External Baffle, L	4.34	3.02	1.32	12.99	13.01	-0.02
#212	#2_External Baffle, U	6.18	2.86	3.32	12.50	12.64	-0.14

^e. Test Result (°C)

^f. Analysis Result (°C)

^g. Deviation (degree °C)

TABLE VII. ON-ORBIT EXPECTED TEMPERATURE RESULT (REVISED)

Requirement	Criteria	Result	Compliance
Cold Balance			
Temperature Normal Deviation			
- Internal Unit	< 5 K	3.35	Complied
- External Unit	< 10 K	4.73	Complied
Temperature Mean Deviation	Less than ±2 K	0.18	Complied

Requirement	Criteria	Result	Compliance
Temperature Standard Deviation	Less than < 3 K	2.51	Complied
Hot Balance			
Temperature Normal Deviation			
- Internal Unit	< 5 K	-	N / A ^h
- External Unit	< 10 K	2.29	Complied
Temperature Mean Deviation	Less than ± 2 K	-0.38	Complied
Temperature Standard Deviation	Less than < 3 K	1.06	Complied

^h. Not Applicable due to No Test Data by Data Loss

The "Bluebon" satellite equipped with the SOP was launched on January 15, 2025, via SpaceX's TR-12 Mission. It was deployed from *LEO Express-2*, which served as *orbital transfer vehicle (OTV)*, and is currently undergoing ADCS commissioning in orbit. The "Bluebon" satellite is scheduled to begin image capturing at a resolution of 5.0 meters in both PAN and MS soon. Through this mission, it aims to demonstrate that high-resolution Earth observation, previously conducted by micro or small satellites, can also be achieved with Nanosatellites, thereby opening up new avenues for the utilization of nanosatellite applications and opportunities.

ACKNOWLEDGMENT

The authors wish to thank "*SatRev*" and "*Impulse Space*" for their support and co-operation for the success of "*Bluebon*" mission.

TelePIX is a leading company in the New Space era, providing EO payloads for the nanosatellite to microsatellite market. For more detailed information, please visit here: <https://telepix.net/>

REFERENCES

- [1] Jin-Soo Chang, Seung-Uk Yang, Yun-Hwang Jeong, Ee-Eul Kim, "Design and Development of Thermal Control Subsystem for an Electro-Optical Camera System", Journal of The Korean Society for Aeronautical and Space Sciences, Vol. 37, No. 8, 2009, pp. 798-804
- [2] Jin-Soo Chang, Jong-Un Kim, Myung-Seok Kang, Seung-Uk Yang, Ee-Eul Kim, "Development and Verification of Thermal Control Subsystem for High Resolution Electro-Optical Camera System, EOS-D Ver.1.0", Journal of The Korean Society for Aeronautical and Space Sciences, Vol. 41, No. 11, 2013, pp. 921-930
- [3] David G. Gilmore, Spacecraft Thermal Control Handbook Second Ed., The Aerospace Press, 2002
- [4] Romain Peyrou-Lauga, "A proposition for updating the environmental standards using real Earth Albedo and Earth IR Flux for Spacecraft Thermal Analysis", 31st European Space Thermal Analysis Workshop, 2017
- [5] xScape100-CMV12000 Imager Electronics - Interface Control Document, Rev. 1, 072501, SIMERA SENSE, 2023
- [6] European Cooperation for Space Standardization, Space product assurance: Derating – EEE components, ESA Requirements and Standards Division, ECSS-Q-ST-30-11C, Rev. 2, 2021
- [7] Jin-Soo Chang, et al. "Preparation and Result Review of Thermal Vacuum Test of Flight Model for Small Electro-Optical Camera by Preceding Thermal Analysis", Proceedings of the 2011 KSAS Fall Conference, Nov. 2011, pp. 1,447-1,451
- [8] European Cooperation for Space Standardization, Space engineering: Thermal control general requirements, ESA Requirements and Standards Division, ECSS-E-ST-31C, Rev. 1, 2008